Journal of Sound and Vibration (2001) **248**(1), 31–42
doi:10.1006/jsvi.2001.3715, available online at http://www.idealibrary.com on IDEAL®

ESTIMATION OF THE HOPF BIFURCATION POINT FOR AEROELASTIC SYSTEMS

A. Sedaghat, J. E. Cooper, A. Y. T. Leung and J. R. Wright

*Dynamics & Aeroelasticity Group, Manchester School of Engineering, Manchester M*13 9*PL, England.*
*E-mail: asedaghat@fs*1.*eng.man.ac.uk*

(*Received* 16 *November* 2000, *and in final form* 22 *February* 2001)

The estimation of the Hopf bifurcation point is an important prerequisite for the non-linear analysis of non-linear instabilities in aircraft using the classical normal form theory. For unsteady transonic aerodynamics, the aeroelastic response is frequency-dependent and therefore a very costly trial-and-error and iterative scheme, frequency-matching, is used to determine flutter conditions. Furthermore, the standard algebraic methods have usually been used for systems not bigger than two degrees of freedom and do not appear to have been applied for frequency-dependent aerodynamics. In this study, a procedure is developed to produce and solve algebraic equations for any order aeroelastic systems, with and without frequency-dependent aerodynamics, to predict the Hopf bifurcation point. The approach performs the computation in a single step using symbolic programming and does not require trial and error and repeated calculations at various speeds required when using classical iterative methods. To investigate the validity of the approach, a Hancock two-degrees-of-freedom aeroelastic wing model and a multi-degree-of-freedom cantilever wind model were studied in depth. Hancock experimental data was used for curve fitting the unsteady aerodynamic damping term as a function of frequency. Fairly close agreement was obtained between the analytical and simulated aeroelastic solutions with and without frequency-dependent aerodynamics.

1. INTRODUCTION

The influence of non-linearities on modern aircraft is becoming increasingly important [1] and the requirement for more accurate predictive tools grows stronger. These non-linearities can be due to structural (free-play, backlash, cubic stiffness), aerodynamic (moving shocks and transonic effects) or control (time delays, control laws) phenomena. The non-linear flutter behaviour such as limit cycle oscillations (LCO) has become of increasing importance over the last few years, although such problems have been noted since the 1970s.

There is an urgent need for a predictive capability of non-linear aeroelastic phenomena. Such ability would enable flight flutter tests to be completed faster and with a greater degree of safety. Although not desirable, LCO is essentially a fatigue problem, whereas flutter is usually catastrophic and must be avoided at all costs. An accurate LCO/flutter prediction capability would reduce significantly the number of flights required in any flight clearance test programme with current costs being estimated at around \$70k per test flight.

There has been much work in recent years [2–4] devoted towards the characterization of non-linear aeroelastic behaviour. This work has primarily consisted of simulating the response of the aeroelastic system through numerical integration, although there are a few known instances of experimental verification [5]. There has also been a significant effort

0022-460X/01/460031 + 12 \$35.00/0

devoted [6, 7] to improving unsteady modelling through the coupling of the aerodynamic and structural models. Significant headway has been made towards solving the problem, particularly in the transonic region. However, there are still major problems inherent due to the enormous computational resources required for even the simplest cases.

A number of mathematical techniques [8–12] exist in the non-linear dynamics community that enable the stability boundaries of a defined non-linear system to be computed and the possible instabilities to be characterized. Normal form theory is the method most used for determining the characteristics of limit cycle oscillations [13–15]. However, estimation of the Hopf bifurcation point is a substantial prerequisite for the normal form theory analysis of non-linear instabilities in aircraft.

Flutter or the Hopf bifurcation point is the condition when an aircraft component (e.g., wing, control surface or tail-plane) exhibits self-sustained divergent oscillations (Dowell *et al.* [16]). The speed at which this occurs is known as the flutter speed. At speeds below the flutter speed, any initial dynamic structural vibrations will be damped, whereas at speeds above the flutter speed any initial dynamic structural disturbance will grow, leading to structural failure if not limited by aerodynamic or structural non-linearity. It is essential that all aircraft be designed such that flutter will not occur. Besides developing sophisticated structural, aerodynamic and aeroelastic mathematical models, a significant degree of testing on the ground and in the air is undertaken to demonstrate that flutter does not occur throughout the desired flight envelope (with a 20% safety margin). Ground vibration and flight flutter tests are mandatory in order to satisfy airworthiness regulations.

Having estimated the mathematical model, the flutter stability of an aircraft is usually examined by calculating the eigenvalues of the state-space form of the aeroelasticity equation at different flight conditions.

In this classical method, the frequency and damping ratio of each of the complex modes derived from the eigenvalue solution are plotted against airspeed (or Mach number). A zero damping value indicates the onset of flutter. For unsteady aerodynamics, the above method is more complicated because a trial-and-error frequency-matching scheme must be used in order to obtain the frequency of the mode that causes flutter to occur.

A simple approach to obtain exact estimates of the flutter frequency and speed for a binary flutter system, based upon the Routh–Hurwitz method, has been known for many years. However, it has not been feasible to use it on larger systems or to include frequency-dependent aerodynamic forces.

In this paper, an approach is developed to calculate the flutter speed and frequency of aeroelastic systems with more than two degrees of freedom (d.o.f.) and also the inclusion of frequency-dependent aerodynamics. A feature of the method is the use of symbolic programming to perform all the calculations. The desired quantities can be determined without the need for iteration. The method is validated using a 2-d.o.f. rectangular wing model, with and without unsteady aerodynamics. A further example, a cantilever wing model, shows the use of the approach on higher order models.

2. FLUTTER CHARACTERISTICS OF A GENERAL 2-d.o.f. SYSTEM

The equations of motion for a general multi-d.o.f. aeroelastic system can be written as

$$\mathbf{M}\ddot{\mathbf{q}} + L\dot{\mathbf{q}} + (\mathbf{K}_{aero} + \mathbf{K}_{struct})\mathbf{q} = 0, \tag{1}$$

where $\mathbf{q}$ is the vector containing the generalized co-ordinates, $\mathbf{M}$ is the mass matrix, $\mathbf{L}$ is the aerodynamic damping and $\mathbf{K}_{aero}$ and $\mathbf{K}_{struct}$ are aerodynamic and structural stiffnesses

respectively. In general, aerodynamic terms can be expressed as functions of the airspeed V and the frequency of vibrations ω. Using the state-space technique for a two-d.o.f. system, the above system may be written in first order form as

$$\begin{bmatrix} \dot{\mathbf{q}} \\ \ddot{\mathbf{q}} \end{bmatrix} = \begin{bmatrix} 0 & I \\ -\mathbf{M}^{-1}(\mathbf{K}_{aero} + \mathbf{K}_{struct}) & -\mathbf{M}^{-1}\mathbf{L} \end{bmatrix} \begin{bmatrix} \dot{\mathbf{q}} \\ \ddot{\mathbf{q}} \end{bmatrix}, \tag{2}$$

where I is a 2×2 identity matrix. Equation (2) is expanded to form a 4×4 matrix system

$$\dot{\mathbf{z}} = \begin{bmatrix} \dot{z}_1 \\ \dot{z}_2 \\ \dot{z}_3 \\ \dot{z}_4 \end{bmatrix} = \begin{bmatrix} \dot{q}_1 \\ \dot{q}_2 \\ \ddot{q}_1 \\ \ddot{q}_2 \end{bmatrix} = \begin{bmatrix} 0 & 0 & 1 & 0 \\ 0 & 0 & 0 & 1 \\ m_{31} & m_{32} & m_{33} & m_{34} \\ m_{41} & m_{42} & m_{43} & m_{44} \end{bmatrix} \begin{bmatrix} z_1 \\ z_2 \\ z_3 \\ z_4 \end{bmatrix}, \tag{3}$$

where the matrix indices m_{ij}, $i = 3, 4$, $j = 1, 2, 3, 4$ are determined based upon the mathematical model used and are functions of the airspeed V and the frequency ω. The corresponding fourth order characteristic polynomial of the system can be written as

$$P(\lambda) = \lambda^4 + a_1\lambda^3 + a_2\lambda^2 + a_3\lambda + a_4 = 0. \tag{4}$$

2.1. ROUTH–HURWITZ APPROACH

Using the classical Routh–Hurwitz approach it can be shown that the critical condition for flutter to occur is

$$a_1a_2a_3 - a_1^2a_4 - a_3^2 = 0, \tag{5}$$

from which the flutter speed can be calculated. The flutter frequency is then found as

$$\omega_F = \sqrt{a_3/a_1}. \tag{6}$$

2.2. SYMBOLIC APPROACH

The characteristic polynomial (4) can be divided by $(\lambda^2 + \omega^2)$ corresponding to double pure imaginary roots, $(\pm i\omega)$, which may correspond to the flutter speed.

$$P(\lambda) = (\lambda^2 + \omega^2)(\lambda^2 + a_1\lambda + (a_2 - \omega^2)) + R, \tag{7}$$

where R, the remainder, is given as

$$R = (a_3 - a_1\omega^2)\lambda + (a_4 - (a_2 - \omega^2)\omega^2). \tag{8}$$

It may be noted that the terms in the remainder R are only a function of the airspeed V and the frequency ω. More importantly, if a physically acceptable solution for airspeed and frequency are found such that the remainder becomes zero, then the characteristic polynomial (4) has double pure imaginary roots $(\pm i\omega)$ corresponding to the Hopf bifurcation point (flutter condition).

This means that at the flutter speed the characteristic polynomial must be divisible by $(\lambda^2 + \omega_F^2)$, which yields the following equations to be solved for the flutter speed V_F and the

flutter frequency ω_F:

$$f_1(\omega_F, V_F) = a_3 - a_1\omega_F^2 = 0, \qquad f_2(\omega_F, V_F) = a_4 - (a_2 - \omega_F^2)\omega_F^2 = 0. \tag{9}$$

The first equation in (9) yields the same flutter frequency as evaluated in equation (6). This method has been programmed using the symbolic programming code Mathematica. Comparison of both approaches for a 2-d.o.f. system shows that exactly the same solution is found using each approach.

3. EXTENSION OF THE METHODOLOGY TO HIGHER ORDER SYSTEMS

It is somewhat complex to extend the application of the Routh–Hurwitz method to higher order aeroelastic systems as the determinants that need to be solved get very complicated and there is no obvious criterion to choose for flutter, unlike the 2-d.o.f. case. However, the extension of the symbolic approach is relatively strightforward.

For example, a 3-d.o.f. system yields the following characteristic polynomial:

$$P(\lambda) = \lambda^6 + a_1\lambda^5 + a_2\lambda^4 + a_3\lambda^3 + a_4\lambda^2 + a_5\lambda + a_6. \tag{10}$$

The sixth order polynomial may be similarly divided by $(\lambda^2 + \omega_F^2)$ to yield the remainder

$$R = (a_5 - \omega_F^2(a_3 - a_1\omega_F^2))\lambda + (a_6 - \omega_F^2(a_4 - \omega_F^2(a_2 - \omega_F^2))) \tag{11}$$

and hence the following set of polynomial equations to be solved for flutter speed and frequency:

$$\begin{aligned} f_1(\omega_F, V_F) &= a_5 - \omega_F^2(a_3 - a_1\omega_F^2) = 0, \\ f_2(\omega_F, V_F) &= a_6 - \omega_F^2(a_4 - \omega_F^2(a_2 - \omega_F^2)) = 0. \end{aligned} \tag{12}$$

In general, for a polynomial of order $2n$, $P_{2n}(\lambda)$, the remainder of division by $(\lambda^2 + \omega_F^2)$ can be written as

$$\begin{aligned} R = (a_{2n-1} - \omega_F^2(a_{2n-3} - \omega_F^2 \cdots (a_3 - a_1\omega_F^2))) \cdots (2n-2)/2\lambda \\ + (a_{2n} - \omega_F^2(a_{2n-2} - \omega_F^2 \cdots (a_2 - \omega_F^2))) \cdots 2n/2. \end{aligned} \tag{13}$$

where the bracket subscripts represent the number of brackets.

4. HANCOCK RECTANGULAR WING MODEL

Consider a rigid wing of constant chord (shown in Figure 1) pivoted at its root in bending γ and torsion θ such that there is no stiffness coupling between the motions (Hancock *et al.* [17]). The equations of motion for the wing model is given by

$$\mathbf{A}\ddot{q} + (\rho V\mathbf{B} + D)\dot{q} + \rho V^2(\mathbf{C} + \mathbf{E})\mathbf{q} = 0 \tag{14}$$

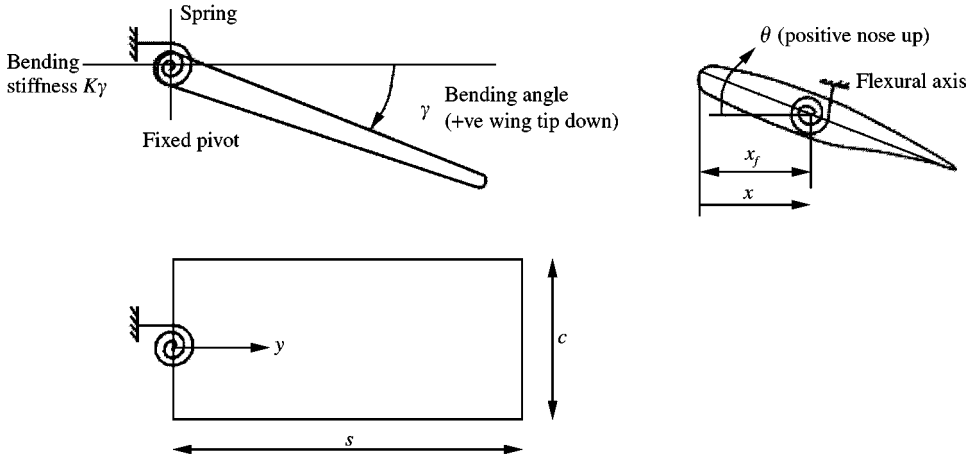

Figure 1. Schematic of the rectangular wing model.

where $\mathbf{q} = (\gamma\ \theta)^{\mathrm{T}}$ is the vector of generalized co-ordinates. For the simple wing model, it can be shown that

$$\mathbf{A} = \begin{bmatrix} I_\gamma & I_{\gamma\theta} \\ I_{\gamma\theta} & I_\theta \end{bmatrix}, \quad \mathbf{B} = \begin{bmatrix} cs^2a/6 & 0 \\ -c^2s^2ea/4 & -(c^3s/2)M_{\dot{\theta}} \end{bmatrix}, \quad \mathbf{C} = \begin{bmatrix} 0 & cs^2a/4 \\ 0 & -c^2sea/2 \end{bmatrix}, \quad \mathbf{E} = \begin{bmatrix} k_\gamma & 0 \\ 0 & k_\theta \end{bmatrix} \tag{15}$$

in which I_γ, I_θ, and $I_{\gamma\theta}$ are the moments of inertia in bending, in pitch and their product, respectively and k_γ, k_θ, are rotational stiffnesses in bending and torsion respectively. The parameters c, s, e and a are the chord length, the wing semi-span, the non-dimensional distance of flexural axis from aerodynamic centre, and the two-dimensional sectional lift curve slope respectively.

In deriving equation (14), quasi-steady aerodynamics was used with the inclusion of the M_θ term, a non-dimensional aerodynamic torsional damping derivative, which is introduced to represent an unsteady aerodynamics effect. The structural damping D has been ignored here; however, it can be included without reducing the generality of the above analysis.

Consider the Hancock wing model shown in Figure 1 with the characteristics: $s = 10\,\mathrm{m}$, $c = 3\,\mathrm{m}$, $x = 0{\cdot}6$ cm, $x_f = 0{\cdot}5$ cm, $m = 200$ kg, $a = 2\pi$, $\rho = 1{\cdot}225\ \mathrm{kg/m^3}$, where m is the mass of the wing and (x_{cm}, y_{cm}) are co-ordinate components of wing centre of mass x_f and a are the distance of the flexural axis from the wing leading edge and two-dimensional lift curve slope respectively. ρ is the air density at zero altitudes. The moments of inertia and stiffness coefficients are determined as

$$I_\gamma = ms^2/3 = 6{\cdot}667 \times 10^3\ (\mathrm{kg\,m^2}),\ I_\theta = mc^2x_{cm}^{2/3} + m(x_{cm} - x_f)^2c^2 = 2{\cdot}8255 \times 10^3\ (\mathrm{kg\,m^2}),$$

$$I_{\gamma\theta} = m(x_{cm} - x_f)0{\cdot}45sc = 8{\cdot}1 \times 10^2\ (\mathrm{kg\,m^2}),\ k_\gamma = (4\pi)^2I_\gamma = 1{\cdot}0528 \times 10^6\ (\mathrm{kg\,m^2/s^2}),$$

$$k_\theta = (20\pi)^2\, mc^2/12 = 5{\cdot}922 \times 10^5\ (\mathrm{kg\,m^2/s^2}). \tag{16}$$

The parameters e, $I_{\gamma\theta}$ and M_θ are varied through the following examples accordingly for different flutter conditions.

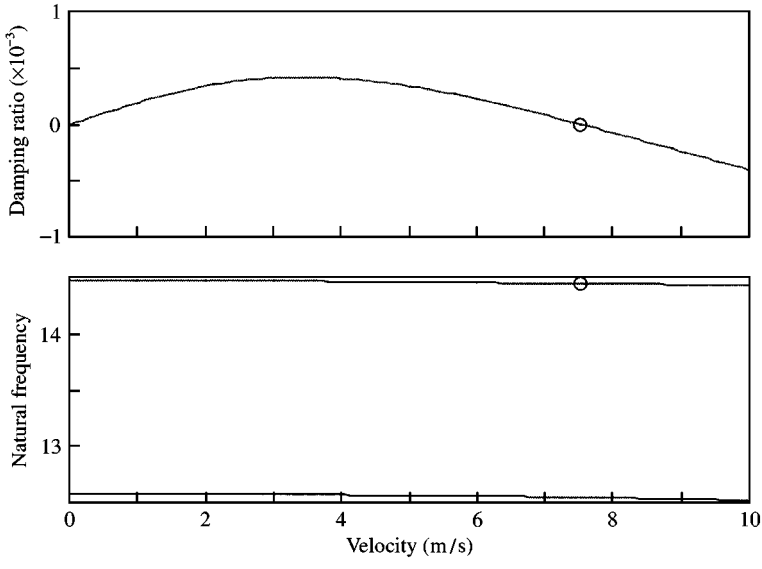

Figure 2. Frequency and damping trends for the case with constant aerodynamics.

4.1. EXAMPLE WITH CONSTANT AERODYNAMICS

Consider the Hancock wing model with the wing mass-balanced (i.e., $I_{\gamma\theta} = 0$), the unsteady aerodynamic damping term set as $M_{\dot{\theta}} = -0{\cdot}1$ and $e = 0{\cdot}25$. Applying the approach developed in this paper leads to the expressions

$$f_1(\omega_F, V_F) = 120{\cdot}909 - 0{\cdot}00442\, V_F^2 - 0{\cdot}583\omega_F^2 = 0,$$

$$f_2(\omega_F, V_F) = 33095{\cdot}9 - 4{\cdot}839\, V_F^2 - 367{\cdot}496\omega_F^2 + 0{\cdot}0273\, V_F^2\omega_F^2 + \omega_F^4 = 0, \tag{17}$$

from which it was found that $\omega_F = 14{\cdot}391$ rad/s and $V_F = 7{\cdot}523$ m/s.

Figure 2 shows the corresponding eigenvalue solution or damping plot for this case. The circles indicate the results found using the symbolic approach. It can be seen that there is an exact agreement between the symbolic and iterative approach.

4.2. EXAMPLE WITH FREQUENCY-DEPENDENT AERODYNAMICS

The next example is an extension of the previous example, where again the wing is mass-balanced about the flexural axis (i.e., $I_{\gamma\theta} = 0$) but now the damping term $M_{\dot{\theta}}$ is assumed to vary depending upon the value of the frequency parameter v. Based upon the values of v given in Hancock *et al.* [17] $M_{\dot{\theta}}$ was curve fitted [18] to obtain the expression

$$(-M_{\dot{\theta}}(v))v = 0{\cdot}491336v/(0{\cdot}1996901 + v). \tag{18}$$

This simple function can be easily inserted into the symbolic approach, and the flutter speed and frequency are found in a single step. A residual between $\pm$ 5% was obtained between the function and the data. This could be reduced if a more complicated curve-fitting expression was used.

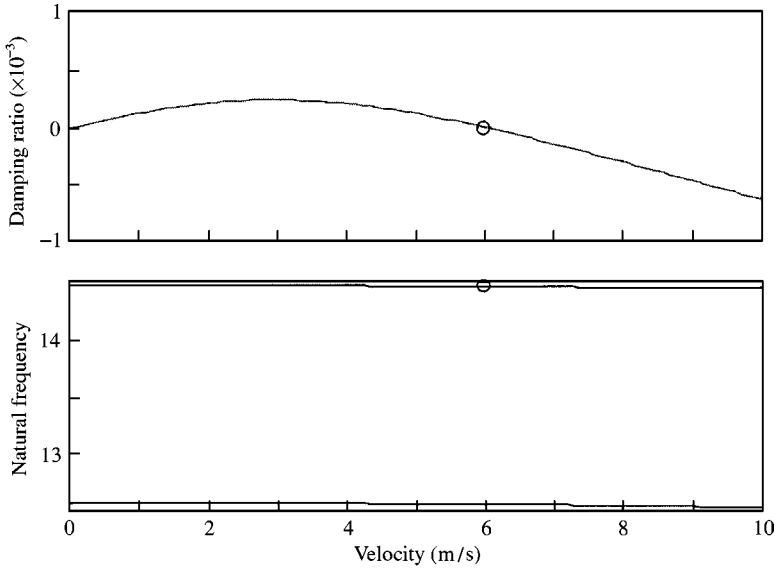

Figure 3. Frequency and damping trends for the case with frequency-dependent aerodynamics (the Hancock wing model with 2-d.o.f.).

The symbolic equations are now found as

$$f_1(v_F, V_F) = 120{\cdot}985 + (4{\cdot}541 - 0{\cdot}0641\,(0{\cdot}223 + v_F)(0{\cdot}05 + 0{\cdot}0264v_F + v_F^2)V_F^2)/$$
$$(0{\cdot}1997 + v_F) = 0,$$
$$f_2(v_F, V_F) = 33095{\cdot}9 - 3{\cdot}9296V_F^2 - 40{\cdot}8329v_F^2V_F^2 + 0{\cdot}00276v_F^2V_F^4$$
$$+ \frac{v_F^4V_F^4}{81} - \frac{0{\cdot}00184v_F^2V_F^4}{0{\cdot}1997 + v_F} = 0 \tag{19}$$

which were solved to give estimates of $\omega_F = 14{\cdot}45$ rad/s and $V_F = 5{\cdot}979$ m/s. Comparison with the eigenvalue solution or damping plot including frequency matching, as shown in Figure 3, again indicates that there is an exact agreement.

5. A CANTILEVER WING MODEL

Consider a simple cantilever wing model, i.e., a uniform flat plate with the thickness t, fixed in at one end but freely unsupported at the other end as shown in the Figure 4. This wing model is used to provide a multi-degree-of-freedom example with possible extension to a more realistic aircraft wing. A Cartesian co-ordinate system is used to describe the wing. According to the Rayleigh–Ritz model, the motion of the wing can be approximated by the summation of a finite number of mode shapes multiplied by the generalized co-ordinates. Here, the bending and torsion modes for the wing are considered where they can be approximated by

$$h = \sum_{i=1}^{m} z^{i+1}q_i, \quad \theta = \sum_{i=1}^{n} z^i q_{m+i}, \tag{20}$$

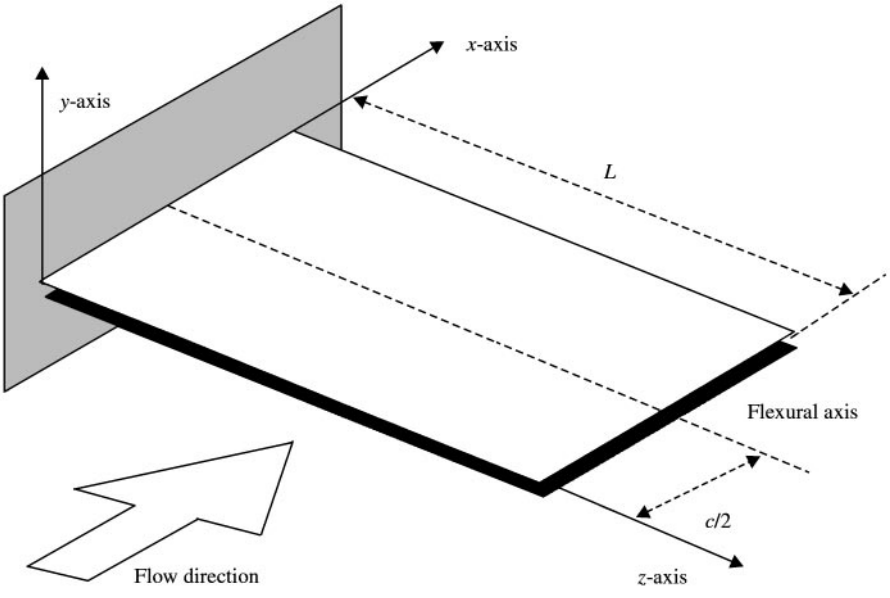

Figure 4. A cantilevered rectangular wing model.

where h is the displacement of the wing tip in the y direction, θ is the rotation of the wing tip along the z-axis, m is the total number of bending modes, and n is the total number of torsion modes.

The Lagrange equation [19] was used for deriving equations of motion and is given by

$$(\mathrm{d}/\mathrm{d}t)(\partial T/\partial \dot{q}_i) + \partial F/\partial \dot{q}_i - \partial T/\partial q_i + \partial V_{PE}/\partial q_i = Q_i, \tag{21}$$

where T is the kinetic energy, V_{PE} the potential energy, F the dissipation force applied to the system, Q_i the ith generalized force and q_i is the ith generalized displacement.

Based on the quasi-steady strip theory and the assumptions made by Dimitriadis [20] for evaluating the system of equations, the expressions were derived for the mass, stiffness, and damping matrices of the wing model (see Sedaghat *et al.* [21]).

5.1. EXAMPLE OF A 3- AND 5-d.o.f. SYSTEMS WITH CONSTANT AERODYNAMICS

Three- and five-d.o.f. aeroelastic systems were created consisting of two bending and one torsion modes, and two bending and three torsion modes of the cantilever wind model respectively. As before, strip theory with the Hancock modification to include unsteady aerodynamics was employed. When the approach developed in this paper was applied to both systems, it was found that for the 3-d.o.f. case $\omega_F = 111{\cdot}23$ rad/s and $V_F = 93{\cdot}94$ m/s, and for the 5-d.o.f. case $\omega_F = 99{\cdot}71$ rad/s and $V_F = 86{\cdot}56$ m/s were predicted based upon the symbolic approach. Figures 5 and 6 show the corresponding eigenvalue solution plots. The flutter speed and frequency are estimated fairly accurately in both cases.

5.2. EXAMPLE OF 3- AND 5-d.o.f. SYSTEMS WITH FREQUENCY-DEPENDENT AERODYNAMICS

As a final example, the same 3- and 5-d.o.f. aeroelastic systems are used as above, but now the damping term $M_{\dot{\theta}}$ is assumed to vary depending upon the value of the frequency

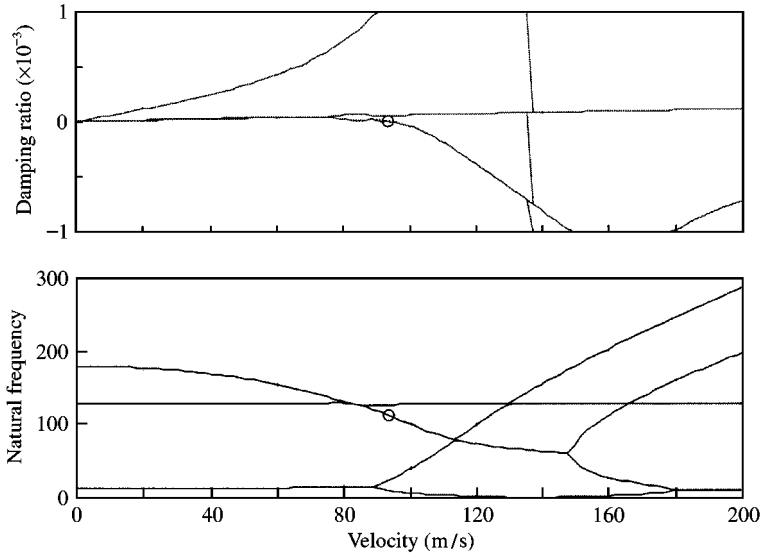

Figure 5. The 3-d.o.f. cantilever wing model with constant quasi-steady aerodynamics ($V_F = 93{\cdot}9415$ m/s, $\omega_F = 111{\cdot}228$ rad/s, $M_{\dot{\theta}} = -0{\cdot}21991$).

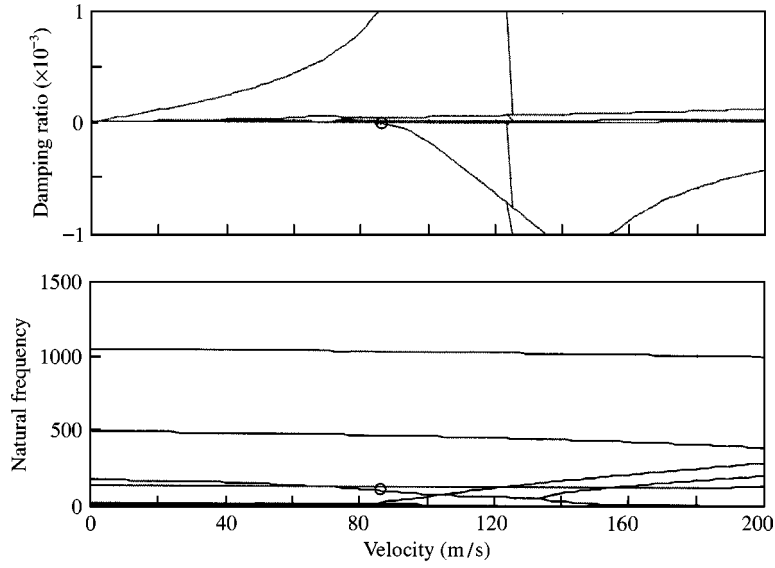

Figure 6. The 5-d.o.f. cantilever wing model with constant quasi-steady aerodynamics ($V_F = 86{\cdot}5602$ m/s, $\omega_F = 99{\cdot}7136$ rad/s, $M_{\dot{\theta}} = -0{\cdot}21991$).

parameter v as is defined in equation (18). For the case with 3-d.o.f. the results outlined below were obtained for the estimation of the bifurcation (flutter) point, which is exactly in agreement with the frequency matching solution shown in Figure 7.

3-*d.o.f. system*: 2 *bending modes*, 1 *torsion mode* $V_F = 105{\cdot}424$ m/s, $v_F = 0{\cdot}245096$, $\omega_F = 86{\cdot}1299$ rad/s, $M_{\dot{\theta}} = -0{\cdot}491336/(0{\cdot}1996901 + v)$, $M_{\dot{\theta}}(v_F) = -1{\cdot}10466$.

Similarly for the case with 5-d.o.f., the approximation outlined below is in very good agreement with the frequency-matching solution shown in Figure 8.

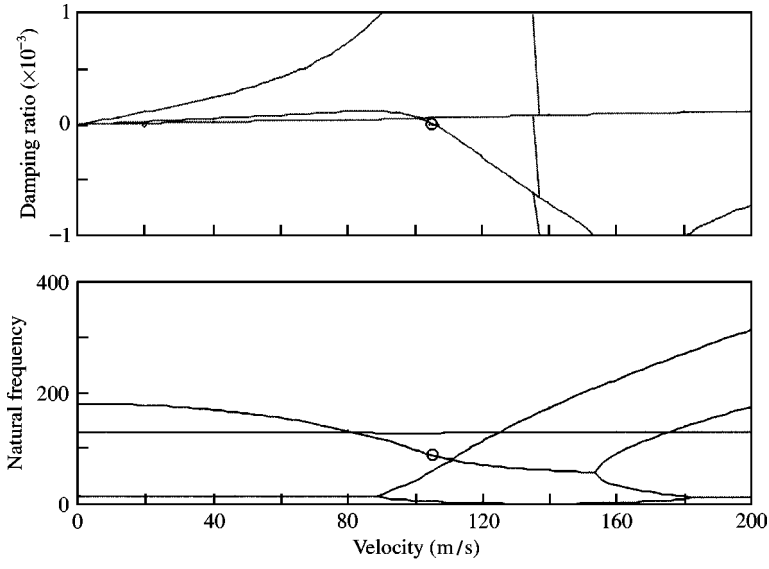

Figure 7. The 3-d.o.f. cantilever wing model with frequency-dependent quasi-steady aerodynamics ($V_F = 105{\cdot}424$ m/s, $v_F = 0{\cdot}245096$, $\omega_F = 86{\cdot}1299$ rad/s, $M_{\dot{\theta}}(v_F) = -1{\cdot}10466$).

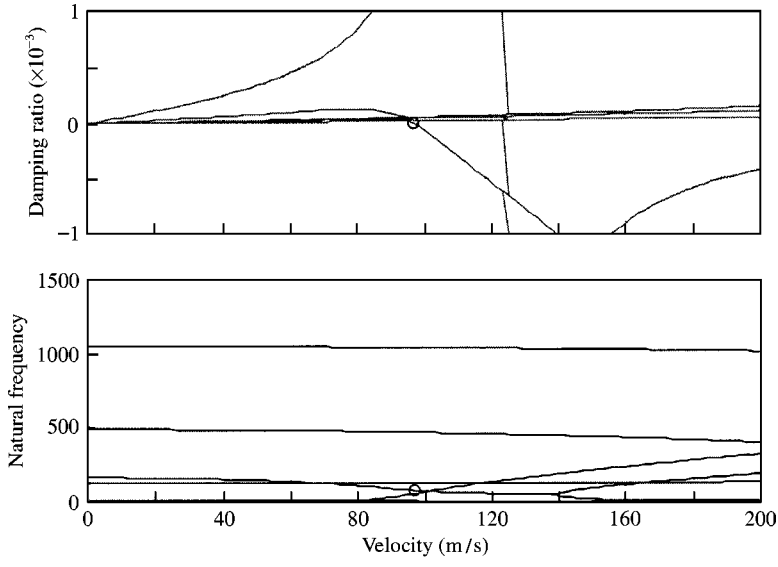

Figure 8. The 3-d.o.f. cantilever wing model with frequency-dependent quasi-steady aerodynamics ($V_F = 96{\cdot}8871$ m/s, $v_F = 0{\cdot}237812$, $\omega_F = 76{\cdot}8031$ rad/s, $M_{\dot{\theta}}(v_F) = -1{\cdot}12305$).

5-d.o.f. system: 2 *bending modes*, 3 *torsion modes* $V_F = 96{\cdot}8871$ m/s, $v_F = 0{\cdot}237812$, $\omega_F = 76{\cdot}8031$ rad/s, $M_{\dot{\theta}} = -0{\cdot}491336/(0{\cdot}1996901 + v)$, $M_{\dot{\theta}}(v_F) = -1{\cdot}12305$.

6. CONCLUSIONS

An approach using symbolic computation has been introduced for calculating the flutter condition of linear multi-d.o.f. aeroelastic systems. The method can be employed to make

the derivation and solution of algebraic equations for any higher order aeroelastic system fairly straightforward. A feature that does not seems feasible for other standard algebraic methods. From the literature, such algebraic capability for aeroelastic systems bigger than 2-d.o.f. including complex unsteady aerodynamics, has not been observed. The need for frequency matching is also eliminated if the unsteady aerodynamics is curve fitted as a function of the frequency parameter. This approach has shown advantages in terms of speed and accuracy, for the test cases studied here, over more traditional methods that calculate a large number of eigenvalues at different airspeeds until the approximate flutter speed and frequency are obtained. The method has been demonstrated successfully on a number of simple aeroelastic systems.

ACKNOWLEDGMENT

This work was supported through an EPSRC Grant GR/L95175.

REFERENCES

1. *AGARD CP*566 1995 Advanced aeroservoelastic testing and data analysis.
2. S. J. Price, H. Alighanbari and B. H. K. Lee 1995 *Journal of Fluid and Structures* **9**, 175–193. The aeroelastic response of a 2 dimensional aerofoil with bilinear and cubic structural non-linearities.
3. G. Dimitriadis and J. E. Cooper 1999 *Aero Journal* **103**, 257–263. Limit cycle oscillation control and suppression.
4. L. Ruiz-Calavera, R. Bannett, J. Fox, X. Huang, I. Kaynes, R. Galbraith, M. Henshaw, P. Nandin, E. Geurts, T. Löser and M. Tamayama 1999 *International Forum on Aeroelasticity and Structural Dynamics*, 1–12. A new compendium of unsteady aerodynamic test cases for CFD.
5. *AGARD CP* 507 1992 Transonic unsteady aerodynamics and aeroelasticity.
6. *AGARD Report* 822 1998 Numerical unsteady aerodynamics and aeroelastic simulation.
7. M. Holden, R. Brazier and A. Cal 1995 *International Forum on Aeroelasticity and Structural Dynamics*, *Paper* 60. Effects of structural non-linearities on a tailplane flutter mode.
8. A. Y. T. Leung and T. C. Fung 1989 *Journal of Sound and Vibration* **131**, 445–455. Construction of chaotic regions.
9. A. Y. T. Leung 1989 *Journal of Sound and Vibration* **131**, 265–273. Stability boundaries for parametrically excited systems by dynamic stiffness.
10. A. Y. T. Leung and T. Ge 1997 *Journal of Sound and Vibration* **202**, 145–160. Normal multi-modes of non-linear Euler beams.
11. A. Y. T. Leung, Q. C. Zhang and Y. S. Chen 1994 *Journal of Shock and Vibration* **1**, 233–240. Normal form analysis of Hopf bifurcation exemplified by Duffing's equation.
12. A. Y. T. Leung and T. Ge 1995 *Journal of Shock and Vibration* **2**, 307–319. An algorithm for higher order Hopf normal form.
13. A. Y. T. Leung and Z. Qichang 1998 *Journal of Sound and Vibration* **217**, 795–806. Higher-order normal form and period averaging.
14. A. Y. T. Leung and T. Ge 1994 *Proceedings of the International Conference on Vibration Engineering ICVE*'94, *Beijing*, 403–408. On the higher order normal form of non-linear oscillators.
15. Y. Chen and A. Y. T. Leung 1999 *Bifurcation and Chaos in Engineering*. Berlin/Heidelberg: Springer-Verlag.
16. E. H. Dowell, E. F. Crawley, H. C. Curtiss Jr, D. A. Peters, R. H. Scanlan and F. E. H. Sisto 1995 *A Modern Course in Aeroelasticity*. Netherlands: Kluwer Academic Publishers; second edition.
17. G. J. Hancock, J. R. Wright and A. Simpson 1985 *The Aeronautical Journal* 285–305, paper 1312. On the teaching of the principles of wing flexure-torsion flutter.
18. A. Sedaghat, J. E. Cooper, A. Y. T. Leung and J. R. Wright 1999 *DYMAC*99: *First International Conference on the Integration of Dynamics*, *Monitoring and Control*, *Manchester*, 1–3 September. Linear flutter prediction using symbolic programming.

19. S. S. RAO 1990 *Mechanical Vibrations*. Reading, MA: Addison-Wesley; second edition.
20. G. DIMITRIADIS 1995 *M.Sc. Thesis, Aerospace Engineering Department. The University of Manchester*, Implementation and comparison of three methods of modelling the effect of the aerodynamic forces on the aeroelastic behaviour of a simple wing.
21. A. SEDAGHAT 1999 *DARG Reports No.* 1, *Dynamics and Aeroelasticity Group, The University of Manchester*. Prediction of aircraft aeroelastic instabilities for non-linear aerodynamics.